

The Good, the Bad, and the Ugly of Markov Boundary for Tabular Prediction

Shu Wan
swan@asu.edu
Arizona State University
Tempe, United States

Abhinav Gorantla
agorant2@asu.edu
Arizona State University
Tempe, United States

Huan Liu
huanliu@asu.edu
Arizona State University
Tempe, United States

K. Selçuk Candan
candan@asu.edu
Arizona State University
Tempe, United States

Abstract

Under standard graphical assumptions, the Markov boundary of a target variable is the smallest set of features that renders every other feature redundant. Once the boundary is observed, the target is conditionally independent of the rest of the table. This is a tempting object for tabular prediction, since it names exactly the columns a model should need. Yet modern regressors are still trained on the full feature set. We ask whether the Markov boundary is genuinely useful for prediction on SCM3K, a 3,450-task synthetic SCM benchmark with feature counts from 40 to 1000 and six SCM families, evaluated with six regressors. The answer is more nuanced than the theory suggests. Restricting a regressor to the oracle boundary often improves prediction substantially, and the improvement grows as the feature space becomes larger and sparser. But the natural pipeline of recovering the boundary with causal discovery and training on the recovered mask does not deliver. Existing estimators exhaust the compute budget before reaching the regime where the boundary helps most, and even where they run they rarely beat the full feature set. We trace this to three causes. Discovery optimizes structural recovery rather than prediction. False negatives and false positives carry sharply asymmetric predictive cost. The exact boundary is only one of many feature sets that beat all features. We then develop what these facts imply for prediction-aligned feature selection and for tabular models that learn to use causal structure.

CCS Concepts

• **Computing methodologies** → **Supervised learning by regression**; *Feature selection*; *Causal reasoning and diagnostics*.

Keywords

Markov boundary, Markov-blanket discovery, tabular prediction, feature selection, causal discovery, structural causal models

ACM Reference Format:

Shu Wan, Abhinav Gorantla, Huan Liu, and K. Selçuk Candan. 2026. The Good, the Bad, and the Ugly of Markov Boundary for Tabular Prediction. In *Proceedings of Proceedings of the 35th ACM International Conference on Information and Knowledge Management (CIKM '26)*. ACM, New York, NY, USA, 11 pages. <https://doi.org/10.1145/nmnnnnn.nmnnnnn>

1 Introduction

The goal of tabular prediction is to estimate a target variable Y from a table of candidate features. Two properties make a feature set ideal for this task. It should be *sufficient*. Conditioning on it

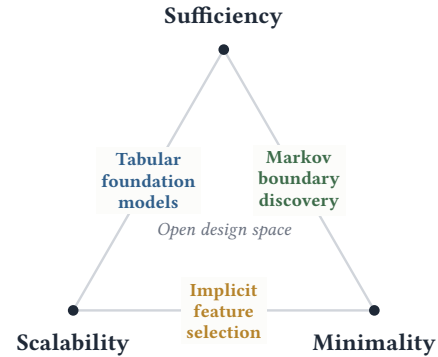


Figure 1: The scalability–minimality–sufficiency triangle for tabular prediction. A good feature set should be sufficient, minimal, and cheap to find. Existing methods often satisfy two of the three goals: Markov boundary discovery is sufficient and minimal but does not scale; implicit feature selection (e.g., LASSO, XGBoost) scales and selects sparse predictors but does not guarantee sufficiency; tabular foundation models (e.g., TabPFN, TabICL) scale and are sufficient but perform no feature selection. The center remains an open design space.

must preserve everything the table reveals about Y , so that no predictive signal is discarded. It should also be *minimal*. It should hold nothing beyond what sufficiency demands, so that the learner is not charged for redundant columns. Causal graphical models give these two properties a single, precise solution. For a target Y in a directed graphical model, the Markov boundary $B(Y)$ consists of its parents, its children, and the other parents of those children. It is the smallest graphical feature set for which Y is conditionally independent of every remaining feature once $B(Y)$ is observed [13, 24]. Under the standard Markov and faithfulness assumptions [25, 32], the boundary is at once minimal and sufficient.

Minimality and sufficiency, however, are not all a practitioner needs. A selection procedure must also be *scalable*. It has to stay tractable as a table widens to hundreds or thousands of columns. On this third axis the comfortable picture breaks. Classical Markov boundary and causal discovery algorithms recover a minimal sufficient set by design, but lean on independence search whose cost grows steeply with the feature count [2, 18, 34]. Models with implicit feature selection, such as the LASSO [33] and tree-based ensembles [5], scale well and select sparse predictors, but their selection follows marginal predictive correlation rather than the conditioning structure, so the retained set need not be sufficient. Figure 1 places these families at the edges of a triangle whose corners are

scalability, minimality, and sufficiency. Each method tends to satisfy two of the three goals.

The remaining case is the regressors that increasingly define tabular prediction. TabPFN and TabICL are transformers pre-trained on millions of synthetic prediction tasks. At test time they ingest an entire table in context and predict without any per-dataset fitting [11, 21, 27]. They are fast, accurate, and scalable, yet by construction they consume every column handed to them. Feature selection is simply not part of the recipe. The model is trusted to discount whatever is irrelevant on its own. Whether that trust is warranted is an empirical question.

This leads us to the central question:

Is the Markov boundary useful for tabular prediction?

If $B(Y)$ is minimal and sufficient, a regressor restricted to $B(Y)$ should lose no predictive information while carrying far fewer columns. But the full table is sufficient too, so population theory alone cannot answer the question. It is a finite-sample claim about how a particular regressor reacts to redundant columns, and it has to be measured.

We measure it with SCM3K¹, a controlled benchmark of 3,450 synthetic SCM tasks. It pairs Erdős–Rényi DAGs with six SCM families. It sweeps the candidate feature count from 40 to 1000 and evaluates six regressors. They include shrinkage baselines, a tree ensemble, a neural network, and tabular foundation models. For every task and regressor we compare the test error of training on all features against training on the oracle Markov boundary, and call their difference the *MB gap*.

The story that emerges is more tangled than the theory predicts. First, the boundary delivers. Restricting to $B(Y)$ improves prediction for most regressors, and the MB gap widens steadily as the feature space grows larger and sparser. Encouraged by this, we test the obvious pipeline. We estimate the boundary with off-the-shelf Markov-boundary and causal discovery, then train on the recovered mask. The result disappoints. The estimators exhaust the compute budget long before reaching the high-dimensional regime where the gap is largest, and even where they do run, the recovered masks rarely beat the full feature set. We then ask why, and find three reasons. Causal discovery optimizes structural recovery, which is not the same objective as prediction. Missing a boundary feature and adding a redundant one are scored identically by recovery metrics, yet they carry sharply asymmetric predictive cost. And the exact boundary is not the only good answer. Many feature sets that differ from $B(Y)$ still beat the full table. The three desiderata of Figure 1 pull against one another exactly in the regime where prediction is hardest.

This is an inconvenient truth, but a generative one. Exact boundary recovery is the objective inherited from causal discovery, but it is the wrong target when the goal is prediction. The evidence points to feature selection that is scalable, prediction-aligned, and willing to trade strict minimality for robustness. We close by developing these implications into concrete directions, from scaling boundary estimation through amortized pre-training to co-learning the feature mask and the predictor together.

Section 2 sets up Markov boundary optimality and the SCM benchmark. Section 3 measures the oracle MB gap. Section 4 tests

the estimate-then-predict pipeline, and Section 5 dissects why it fails. Section 6 characterizes prediction-useful feature sets beyond the exact boundary. Section 7 develops the implications into research directions, Section 8 situates the paper, and Section 9 concludes.

2 Preliminaries

2.1 Markov boundary fundamentals

Let $\mathbf{X} = (X_1, \dots, X_F)$ be the candidate features and let Y be the regression target. For $S \subseteq [F]$, write \mathbf{X}_S for the restricted feature vector and define the population squared-loss risk

$$R^*(S) = \mathbb{E}[(Y - \mathbb{E}[Y | \mathbf{X}_S])^2]. \quad (1)$$

We call S *Bayes sufficient* when $R^*(S) = R^*([F])$.

For a DAG \mathcal{G} over $\{Y, X_1, \dots, X_F\}$, the graphical Markov boundary of Y is

$$B \equiv B(Y) = \text{Pa}(Y) \cup \text{Ch}(Y) \cup \text{Sp}(Y), \quad (2)$$

where $\text{Sp}(Y)$ are the other parents of Y 's children. We write $k = |B|$, $\rho = k/F$ for the boundary fraction, and $\text{redundancy_ratio} = 1 - \rho$ in the empirical models.

Assumption 2.1 (Weak predictive faithfulness). The data distribution is positive, Markov, and faithful to a DAG \mathcal{G} over Y and the features. The same DAG \mathcal{G} governs the training and test distributions, so the Markov boundary of Y is invariant across the train/test split. For every proper subset $S \subsetneq B(Y)$,

$$\mathbb{P}(\mathbb{E}[Y | \mathbf{X}_S] \neq \mathbb{E}[Y | \mathbf{X}_B]) > 0. \quad (3)$$

This condition is natural whenever every boundary variable contributes to the conditional mean of Y . It can fail when a variable affects only higher moments of $Y | \mathbf{X}_B$, such as the noise variance but not the conditional expectation. The heteroskedastic SCM family in SCM3K can violate this condition; we retain it as an empirical robustness check rather than a setting where the theory applies.

Theorem 2.2 (Boundary sufficiency and internal minimality). *Under Theorem 2.1, $B(Y)$ is Bayes sufficient and no proper subset of $B(Y)$ is Bayes sufficient. In particular,*

$$R^*(B) = R^*([F]), \quad (4)$$

and $R^*(S) > R^*(B)$ for every $S \subsetneq B$.

PROOF. The Markov-boundary separator property gives $Y \perp\!\!\!\perp \mathbf{X}_{[F] \setminus B} | \mathbf{X}_B$. Hence $\mathbb{E}[Y | \mathbf{X}_{[F]}] = \mathbb{E}[Y | \mathbf{X}_B]$, and the population risks coincide: $R^*(B) = R^*([F])$. Now let $S \subsetneq B$. By Equation (3), $\mathbb{E}[Y | \mathbf{X}_S] \neq \mathbb{E}[Y | \mathbf{X}_B]$ with positive probability, so the conditional mean changes and $R^*(S) > R^*(B)$. \square

Corollary 2.3 (All features are also sufficient). *The full feature set $[F]$ is Bayes sufficient. Population sufficiency alone therefore does not distinguish B from $[F]$.*

2.2 SCM3K benchmark dataset

SCM3K is a family of 3,450 synthetic SCM tasks. Each split fixes $F \in \{40, 60, 80, 100, 200, 400, 600, 800, 1000\}$, sets the DAG size to $F + 1$ nodes, and treats one node as the target. Low-dimensional splits ($F \leq 100$) use dense Erdős–Rényi graphs with densities 0.2 and 0.4,

¹<https://huggingface.co/datasets/CSE472-blanket-challenge/SCM3K>

Table 1: SCM3K benchmark used throughout the paper. The dense splits are low-dimensional negative controls. The sparse splits create the high-dimensional redundant regime where the MB gap is expected to be visible.

Splits	DAG density	MB-ratio band	Tasks per F
$F \leq 100$	{0.2, 0.4}	[0.10, 0.90]	300
$F \geq 200$	{0.01, 0.02, 0.04}	[0.05, 0.95]	450

with target MB-ratio band [0.10, 0.90]. Higher-dimensional splits use sparse graphs with densities 0.01, 0.02, and 0.04, with band [0.05, 0.95] [7].

Each DAG is paired with six SCM families. They are linear Gaussian, linear non-Gaussian, additive Gaussian, additive non-Gaussian, post-nonlinear, and heteroskedastic. Each task has $n = 1000$ samples, $\text{coeff_range} = 1.0$, and $\text{noise_std} = 0.5$. Nodes are generated in topological order and standardized after assignment, following the benchmark generator’s anti-varsortability convention [29]. The target is selected by the MB-ratio band alone. Parentless targets may qualify, but empty boundaries are excluded by the lower bound. Table 1 summarizes the split design.

2.3 Prediction quantities

For a fixed regressor R and feature subset S , let $\text{RMSE}_R(S)$ be the test RMSE when R is trained and queried using only X_S . The absolute and relative MB gaps are

$$\Delta_{\text{MB}}(R) = \text{RMSE}_R([F]) - \text{RMSE}_R(B), \quad (5)$$

$$\delta_{\text{MB}}(R) = \Delta_{\text{MB}}(R)/\text{RMSE}_R([F]). \quad (6)$$

Positive values mean that the oracle boundary improves prediction over all features. For estimated masks \widehat{S} , we use the same prediction gain scale.

$$\text{prediction_gain}(\widehat{S}) = \text{RMSE}_R([F]) - \text{RMSE}_R(\widehat{S}). \quad (7)$$

Precision, recall, false positives, and false negatives are always computed against the oracle boundary B .

3 When the Boundary Helps

The Markov boundary is a useful prediction oracle. The oracle gain is finite-sample and regressor-dependent. It grows when redundant dimensions stress the downstream regressor, and it shrinks when the regressor already performs feature selection.

3.1 Cross-regressor MB gap

We evaluate six regressors on SCM3K. Ridge and LASSO are shrinkage baselines [10, 33]. MLP and XGBoost cover nonlinear neural and tree-boosting regressors [5, 12]. TabPFN and TabICL represent prior-fitted tabular foundation regressors [11, 27, 28]. Across these six regressors, the median relative oracle RMSE reduction is strongly regressor-dependent. The median reductions are Ridge +35%, MLP +24%, TabICL +18%, TabPFN +12%, XGBoost +4%, and LASSO +2%. The qualitative pattern is stable across the F sweep. The gap is small below $F = 200$ and in relatively dense graphs. It is largest when the full feature set is high-dimensional and redundant. Figure 2 reports this pattern across the six regressors.

Implicit feature selection explains the small-gap end of the spectrum. LASSO explicitly sparsifies. XGBoost selects split variables. Their small oracle gaps therefore do not mean feature selection is unimportant. They mean the feature-selection burden has already been partly absorbed by the regressor. TabPFN and TabICL still show nontrivial oracle gaps, including cases above a 10% prediction-loss change, so tabular foundation model regressors are not immune to redundant features.

3.2 MB gap attribution

We summarize the cross-regressor effect with the final attribution model on relative MB gap. Mixed-effect models are the standard reference point for repeated or grouped observations [14]. Here we report the fixed-effect attribution form because the paper uses the model only to summarize factor effects.

$$\begin{aligned} \delta_{\text{MB}} \sim & \text{redundancy_ratio} + \log_{10} F + \text{scm_family} + \text{regressor} \\ & + \text{regressor} : \text{redundancy_ratio} + \text{regressor} : \log_{10} F. \end{aligned} \quad (8)$$

We report this final specification directly in the main body. The model-selection ladder is not needed for the core argument. If space allows, it can move to an appendix. Figure 3 visualizes the fitted marginal effects.

The model confirms the visual pattern. Redundancy and regressor identity are the strongest factors. Density is largely the same signal as redundancy with the opposite sign. SCM family is weak after these covariates are included. In univariate checks, redundancy ratio and regressor identity are effectively tied for the largest adjusted R^2 values (0.221 and 0.219), followed by density (0.187) and $\log_{10} F$ (0.166). SCM family explains much less (0.012). This is the main empirical message of Section 3. The MB gap is not a property of the graph alone, or of the regressor alone, but of their interaction at a fixed sample budget.

3.3 A finite-sample explanation

The population theorem says that both B and $[F]$ are sufficient. The finite-sample question is how much variance the learner pays for using unnecessary columns. A linear Gaussian SCM gives the simplest example of this effect.

Assumption 3.1 (Linear Gaussian working model). For the purpose of this approximation only, suppose that the conditional model is correctly specified and linear, the features have an arbitrary positive-definite covariance Σ_S that is the same in the training and test distributions, the noise variance is σ^2 , and $n > p + 1$ where $p = |S|$.

Proposition 3.2 (Finite-sample MB gap). *Under Theorem 3.1, for any Bayes-sufficient subset S with $p = |S|$,*

$$\mathbb{E}\left[R(\widehat{\beta}_S)\right] = R^*(B) + \frac{\sigma^2 p}{n - p - 1}. \quad (9)$$

In particular, the full-vs-boundary gap is

$$\frac{\sigma^2 F}{n - F - 1} - \frac{\sigma^2 k}{n - k - 1} = \frac{\sigma^2 (F - k)}{n} + O\left(\frac{F^2 + k^2}{n^2}\right). \quad (10)$$

PROOF. For any Bayes-sufficient subset S , the linear conditional mean is correctly specified in this model. The OLS estimator $\widehat{\beta}_S$

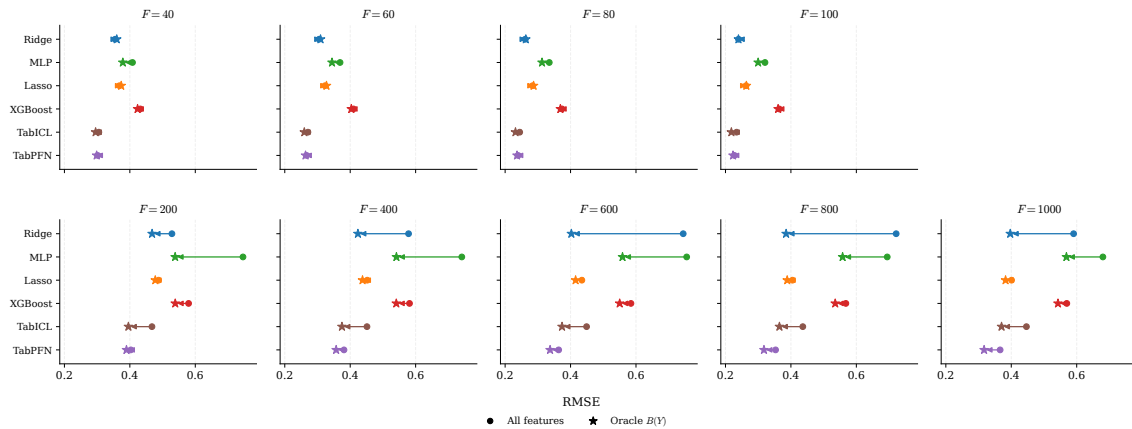


Figure 2: Oracle MB gap by downstream regressor. The boundary helps most for regressors that pay a high finite-sample cost for extra columns, and least for models with strong implicit feature selection.

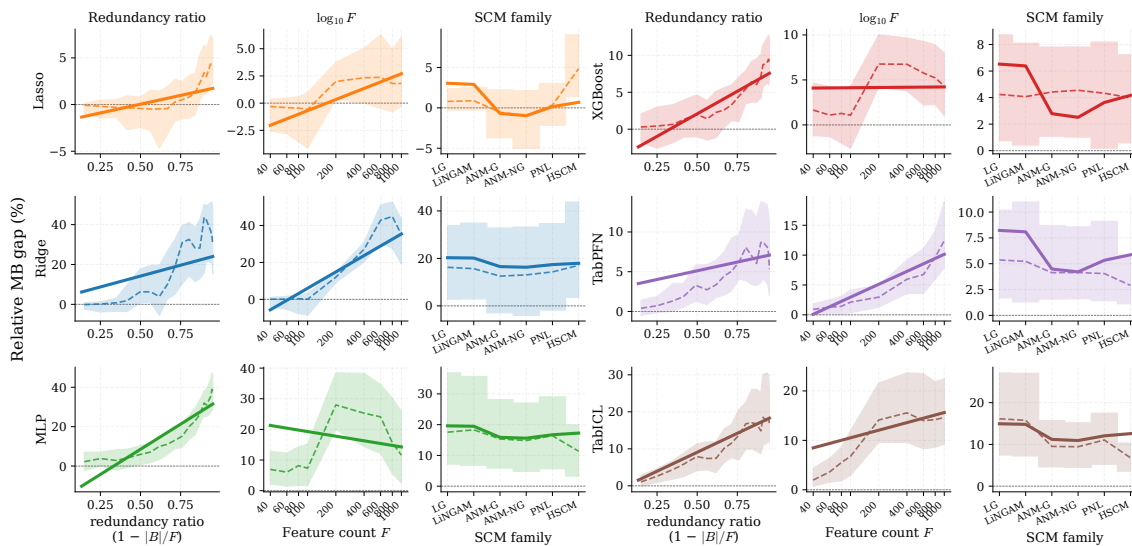


Figure 3: Regressor-conditioned attribution of the MB gap. The gap is explained primarily by redundancy, feature dimension, and regressor identity. SCM family contributes little after these factors are controlled.

is unbiased, so the excess test risk above $R^*(B)$ is pure estimation variance. Under Gaussian errors with a fixed positive-definite design covariance, the prediction variance of OLS on p regressors with n observations follows the Wishart distribution, giving $\mathbb{E}[R(\hat{\beta}_S)] = R^*(B) + \sigma^2 p / (n - p - 1)$ [9]. Both B and $[F]$ are sufficient, but they fit k and F coefficients respectively. Subtracting gives the exact gap. A Taylor expansion in $1/n$ yields the leading term $\sigma^2(F - k)/n$. \square

The gap is the variance cost of estimating $F - k$ extra coefficients whose population contribution is zero once B is observed. This expression is exact for OLS under the Gaussian model, but it is not meant to cover every regressor. When p approaches or exceeds n , OLS is no longer the right working model. Regularized

and nonlinear regressors replace raw parameter count with effective complexity, and their finite-sample cost for redundant features depends on the specific inductive bias. That is exactly what Equation (8) captures through regressor-specific slopes.

4 The Emperor’s New Blanket

Oracle boundaries can improve prediction, but current causal estimators rarely turn that advantage into prediction gains.

The natural recipe is simple. Estimate the Markov boundary, restrict the table to that estimated mask, and train the same downstream regressor. We test this recipe with three unsupervised causal estimators. GES is a score-search method [6]. Grow-Shrink is a local boundary estimator [18]. HITON-MB follows the same local discovery tradition [2].

Table 2: Causal Markov-boundary estimators are accurate only in the low- to mid-dimensional regime and do not reliably improve prediction. F1, precision, recall, wall time, and completion are method-level recovery statistics. Win rates are downstream prediction wins against the all-feature baseline for each regressor. Missing cells are shown as ‘-’.

F	Method	F1	Prec.	Recall	Win/Ridge	Win/TabPFN	Win/XGB	Time (s)	Completion
40	GES	0.438	0.826	0.330	6.7%	1.1%	13.6%	162.1	98.9%
	Grow-Shrink	0.737	0.844	0.691	48.6%	20.7%	48.6%	10.9	99.4%
	HITON-MB	0.523	0.764	0.432	10.5%	5.0%	25.3%	18.0	100.0%
60	GES	0.339	0.875	0.228	4.3%	0.0%	9.2%	278.7	76.7%
	Grow-Shrink	0.688	0.861	0.606	55.3%	16.2%	46.4%	9.5	99.4%
	HITON-MB	0.451	0.791	0.343	6.9%	0.0%	19.8%	22.1	98.3%
80	GES	0.214	0.824	0.138	0.0%	0.0%	0.0%	475.1	9.4%
	Grow-Shrink	0.652	0.820	0.585	58.7%	22.2%	51.7%	9.3	100.0%
	HITON-MB	0.392	0.734	0.287	5.2%	0.0%	28.6%	19.0	97.8%
100	GES	-	-	-	-	-	-	-	-
	Grow-Shrink	0.623	0.711	0.610	35.4%	39.1%	43.8%	9.4	99.4%
	HITON-MB	0.253	0.576	0.180	1.7%	0.0%	8.3%	16.2	100.0%
200	GES	-	-	-	-	-	-	-	-
	Grow-Shrink	0.633	0.570	0.752	98.9%	37.4%	77.9%	8.1	100.0%
	HITON-MB	0.588	0.818	0.485	58.0%	1.1%	55.8%	8.0	98.9%

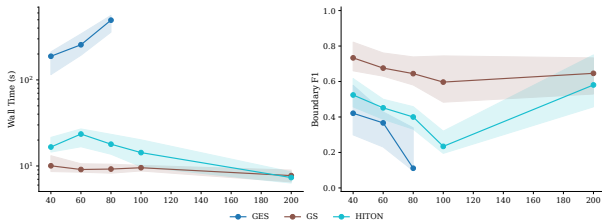


Figure 4: Causal boundary estimators are least available where the oracle MB gap is largest. GES times out beyond small F . GS and HITON-MB are capped around $F = 200$.

The recovery results are not enough to support the oracle story. Grow-Shrink is the most reliable of the three up to $F = 200$. HITON-MB has high precision but low recall. GES has high precision but very low recall and becomes unusable past $F = 80$ under the SCM3K budget. GES completion falls to 9.4% at $F = 80$ and 0% at $F = 100$. Grow-Shrink reaches $F = 200$ with mean F1 0.633, while HITON-MB reaches $F = 200$ with mean F1 0.588 but recall only 0.485. These are precisely the feature sizes below or near the region where the oracle MB gap is still limited. Figure 4 and Table 2 show the resulting scale mismatch.

The same table also shows a precision-oriented failure mode. Causal recovery methods, especially local constraint-based methods, often prefer conservative blankets with higher precision than recall. HITON-MB has higher precision than recall at every evaluated feature count, and Grow-Shrink is precision-heavy through $F = 100$ before flipping at $F = 200$. This matters for prediction because the next section shows that false negatives are usually more costly than false positives.

The downstream prediction outcome also depends on the regressor. Ridge benefits most from masks because it has little built-in feature selection. XGBoost benefits less because split selection already filters many irrelevant variables. TabPFN often loses under estimated masks, despite its nonzero oracle MB gap, indicating that noisy masks can remove useful context even when the true boundary would help. For example, Grow-Shrink reaches 98.9% wins for Ridge at $F = 200$, but only 37.4% for TabPFN at the same split. HITON-MB wins at most 5.0% of TabPFN tasks. The paired recovery and win-rate columns in Table 2 show this failure directly. This section stops at the empirical failure. The next section explains why the failure is structural.

5 Failure Mechanisms

5.1 Scalability

Causal estimators struggle to reach the regime where the oracle MB gap is largest.

The scale problem is not merely implementation overhead. Local constraint-based methods perform conditional-independence tests over candidate neighborhoods. In the worst case, conditioning sets up to size d induce $O(F^d)$ candidate tests. This is the same combinatorial pressure that appears throughout constraint-based structure learning [1, 34, 35, 41]. Score-search methods avoid the same test enumeration but still search over a rapidly growing graph space.

Empirically, this complexity meets SCM3K exactly where it hurts. GES is effectively limited to $F \leq 80$ under the run budget, while Grow-Shrink and HITON-MB are capped around $F = 200$. Section 3 showed that the oracle gap is small below $F = 200$ and grows in higher-dimensional redundant settings. The available

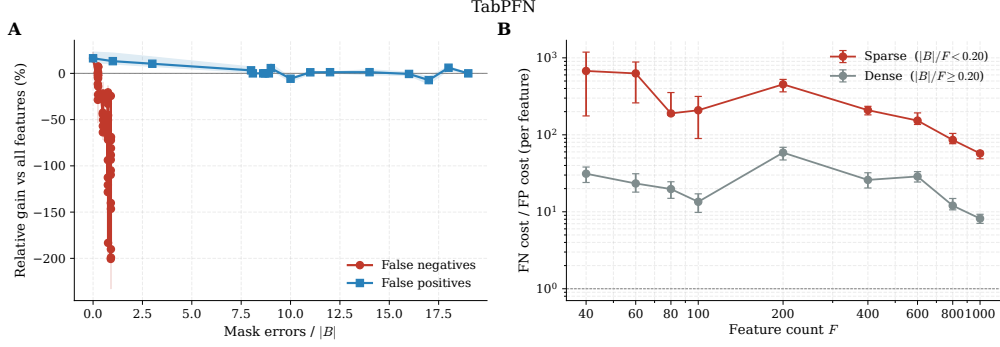


Figure 5: False negatives and false positives have different downstream costs. The TabPFN panel shown here follows the same qualitative asymmetry as the other regressors. Missing boundary variables change the conditional predictor, while adding redundant variables mainly changes finite-sample variance.

causal estimators therefore operate mostly where the prediction reward is weakest.

5.2 Asymmetric loss

Exact-boundary metrics treat false positives and false negatives as identification errors, but prediction risk weights them very differently.

We perturb the oracle boundary directly to isolate the two error types. A false negative removes a true boundary feature. A false positive keeps the boundary intact but adds a non-boundary feature. Across regressors, the model-free per-feature cost ratio $\alpha_{\text{FN}}/\alpha_{\text{FP}}$ is greater than one in every reported cell. The magnitude is regressor-dependent. LASSO ratios are large because the FP cost is nearly zero. Ridge ratios shrink with F as extra columns become costly. TabPFN gives the canonical asymmetric pattern. It has large FN cost and moderate FP cost. Figure 5 summarizes the perturbation experiment.

The asymmetry is the omitted-variable-bias story in predictive form. Let \hat{S} be an estimated mask, $\Delta^+ = \hat{S} \setminus B$, and $\Delta^- = B \setminus \hat{S}$.

Proposition 5.1 (Mask-error decomposition). *Under the linear Gaussian model of Theorem 3.1, adding $s^+ = |\Delta^+|$ redundant variables to a mask that contains B preserves the population predictor. Its leading cost is an additional variance term of order $\sigma^2 s^+ / n$. Omitting boundary variables introduces a population-risk term that does not vanish as n grows. Write $M = \hat{S}$ and $O = B \setminus M$; then*

$$R^*(M) = R^*(B) + \mathbb{E} \left[(\mathbf{X}_O^\top \beta_O - \mathbb{E}[\mathbf{X}_O^\top \beta_O | \mathbf{X}_M])^2 \right]. \quad (11)$$

PROOF. If $\hat{S} \supseteq B$, the Markov-boundary separator property gives $Y \perp\!\!\!\perp \mathbf{X}_{[F] \setminus \hat{S}} | \mathbf{X}_{\hat{S}}$. Consequently, $\mathbb{E}[Y | \mathbf{X}_{\hat{S}}] = \mathbb{E}[Y | \mathbf{X}_B]$ in population. The extra coordinates in Δ^+ have zero population contribution once B is conditioned on. They can still increase finite-sample error because their coefficients must be estimated, giving the leading $\sigma^2 s^+ / n$ variance cost under the linear Gaussian model.

Now suppose \hat{S} omits at least one boundary variable. Write $M = \hat{S}$ and $O = B \setminus M$. Under the linear Gaussian model, the target can

be written as

$$Y = \mathbf{X}_M^\top \beta_M + \mathbf{X}_O^\top \beta_O + \varepsilon, \quad \mathbb{E}[\varepsilon | \mathbf{X}_M, \mathbf{X}_O] = 0.$$

The best predictor from \mathbf{X}_M alone is $\mathbb{E}[Y | \mathbf{X}_M] = \mathbf{X}_M^\top \beta_M + \mathbb{E}[\mathbf{X}_O^\top \beta_O | \mathbf{X}_M]$. The residual $\mathbf{X}_O^\top \beta_O - \mathbb{E}[\mathbf{X}_O^\top \beta_O | \mathbf{X}_M]$ is the component of the omitted signal that \mathbf{X}_M cannot recover, and its expected squared magnitude is the population-risk penalty in Equation (11). This term does not vanish with more samples [9, 38]. \square

Thus a high-precision, low-recall boundary estimator can look reasonable under exact-recovery metrics while still damaging prediction. This explains why F1, SHD, or constraint satisfaction are incomplete objectives for tabular prediction.

5.3 Minimality

The exact Markov boundary is the minimal sufficient set, not the only prediction-relevant set.

Theoretical optimality singles out B because it is minimal. For prediction, however, minimality is only one part of the story. Any controlled superset of B preserves the population conditional and may be preferable to a brittle estimate that misses boundary variables.

Proposition 5.2 (Superset sufficiency). *If $S \supseteq B$, then S is a Markov blanket of Y and $R^*(S) = R^*(B)$.*

PROOF. Write $C = S \setminus B$ and $T = [F] \setminus S$. The graphical Markov-boundary property gives $Y \perp\!\!\!\perp (X_C, X_T) | X_B$. By weak union, $Y \perp\!\!\!\perp X_T | X_B, X_C$, so S is a Markov blanket and $\mathbb{E}[Y | \mathbf{X}_S] = \mathbb{E}[Y | \mathbf{X}_B]$. The risk equality $R^*(S) = R^*(B)$ follows directly. \square

This proposition does not claim that larger masks beat the oracle boundary. It says that exact recovery is too narrow as a training or evaluation target. Over-inclusive masks may lose finite-sample efficiency, but they can still be much safer than masks that drop boundary variables. This motivates the prediction-aligned view in the next section.

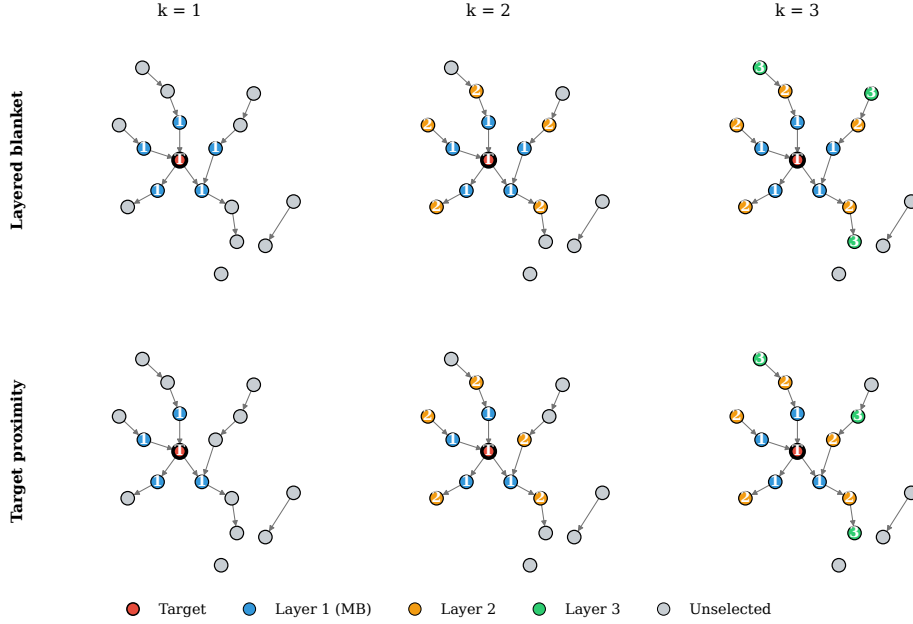


Figure 6: Layered blankets versus target proximity as mask families. The top row expands by accumulated Markov-boundary layers, while the bottom row expands by shortest-path distance from the target. The two constructions can include different nodes at the same rank, even on the same DAG.

6 Beyond the Boundary

The previous sections explain why exact MB recovery is a poor proxy for prediction. This raises the question the rest of the paper turns on. If the exact boundary is not the right target, what makes a feature set *good* and *useful* for prediction? We answer it constructively with two computation-only devices. The first is layered blankets. The second is a prediction gain map over mask precision and recall. We then state the prediction-aligned object directly.

6.1 Layered blankets

Let $B(v)$ denote the Markov boundary of node v in the full DAG. Define accumulated layers

$$L_{\leq 1} = B(Y), \quad L_{\leq k+1} = \left(L_{\leq k} \cup \bigcup_{v \in L_{\leq k}} B(v) \right) \setminus \{Y\}. \quad (12)$$

The associated blanket rank $\kappa(v)$ is the first k such that $v \in L_{\leq k}$, with disconnected nodes assigned an infinite rank. The comparison baseline is target proximity, the shortest-path distance from Y in the undirected skeleton. Figure 6 contrasts these two expansions. Layered blankets follow Markov-boundary closure, while target proximity follows graph distance from Y . The two already differ at rank one, and the difference is exactly the Markov property. Layered@1 is the Markov boundary $B(Y)$ itself. Proximity@1 collects only the immediate skeleton neighbors of Y , namely its parents and children. Spouses lie two hops away in the skeleton. They are reachable only through a shared child. Proximity@1 therefore

omits them and is not a Markov blanket. The comparison that follows therefore isolates the predictive cost of dropping spouses, that is, of breaking the Markov property by a single structural step.

Proposition 6.1 (Layered blankets are over-inclusive blankets). *Every accumulated layer $L_{\leq k}$ is a Markov blanket of Y .*

PROOF. Each $L_{\leq k}$ contains $B(Y)$. The result follows immediately from Theorem 5.2. \square

Empirically, $L_{\leq 1} = B(Y)$ is the peak for every F , as expected. It is the oracle boundary. Later layers dilute the oracle. The value of the layered construction is not that larger layers outperform B , but that they expose structured over-inclusive masks and separate boundary-aware expansion from plain graph distance. For TabPFN, layered@1 is substantially better than target-proximity@1 for $F = 200$ –800. The margin ranges from +10.8 to +20.9 percentage points over this high-dimensional band. Ridge shows the same boundary-aware advantage at every F split, with margins from +9.9 to +17.0 percentage points. Because layered@1 and proximity@1 differ in that proximity can omit the non-adjacent spouses of Y , this margin is precisely the predictive price of dropping them. A mask that breaks the Markov property by a single structural step gives up a large, regressor-independent amount of accuracy. Preserving the Markov property means including spouses. That is what makes a feature set useful, not mere proximity to the target. Figure 7 reports the layered comparison in absolute RMSE for TabPFN.

6.2 Prediction gain maps

Section 6.1 established that the exact boundary is not the only feature set worth having. For $k > 1$, layered blankets are generally

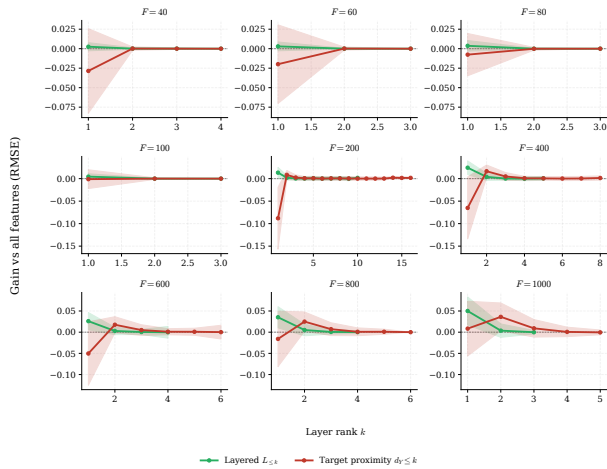


Figure 7: Test RMSE of two mask-expansion strategies for TabPFN: layered blankets (Markov-boundary closure) versus target proximity (graph distance). At rank one, proximity can omit non-adjacent spouses, and the gap shows their predictive cost. Adding further layers dilutes the boundary for both strategies.

over-inclusive supersets of $B(Y)$, and they can still beat the full feature set. That turns a yes/no question into a quantitative one. Across the whole space of candidate masks, which ones are good, and what property makes them good? We go one step beyond Section 6.1 and characterize good masks directly, rather than enumerate them.

To keep the characterization clean we hold two things fixed. We condition on a single feature count F and a single downstream regressor, so that the only quantity varying is the *composition* of the mask itself. Each panel of Figure 8 simply repeats the analysis for one regressor. A mask is then described by how it differs from the oracle boundary. Its true positives (boundary features kept), false negatives (boundary features dropped), and false positives (non-boundary features added). On controlled perturbations of B we fit a simple model of prediction gain,

$$\text{prediction_gain} \sim \text{tp_count} + \text{fn_count} + \text{fp_count}/n, \quad (13)$$

The three coefficients serve as a local, regressor-conditioned diagnostic. A good blanket is one whose true-positive, false-negative, and false-positive counts place it on the winning side of the fitted model. The map is descriptive, not a universal mask-risk law: it summarizes how a particular regressor responds to mask composition at a fixed feature count.

To read the model in the more familiar precision–recall coordinates, note that at a precision–recall pair (π, r) the implied counts are

$$\text{fn} = (1 - r)|B|, \quad (14)$$

$$\text{fp} = r|B|(1/\pi - 1). \quad (15)$$

Substituting these into Equation (13) turns it into a map over (π, r) . Masks above the zero contour are predicted to beat all features, and masks below it are not. Figure 8 draws this *prediction-useful region*.

It is a concrete description of what a good blanket looks like for a given regressor.

The two overlaid trajectories place the mask families from Section 6.1 on this plane. The blue layered path starts at the top-right oracle point. It stays on the recall-one edge because every layered mask contains $B(Y)$, so increasing k only adds variables outside the boundary. The brown proximity path starts from direct skeleton neighbors of Y . That first mask excludes spouses, so recall is low and the predicted gain is poor. Larger radii repair the false negatives, but they also add many false positives. This mirrors the actual layered-curve results. Layered@1 is the oracle peak, while proximity@1 underperforms in the same regimes. The prediction gain map is therefore a useful local approximation of the empirical mask-family landscape, not only a fitted contour.

The region is wide, and it is not the same for every regressor. The fitted TabPFN map has $R^2 = 0.758$ with a strong negative coefficient for missed boundary features. The Ridge map has lower $R^2 = 0.436$ and a much larger false-positive penalty, reflecting Ridge’s sensitivity to redundant columns. The prediction gain map also makes the false-positive and false-negative tradeoff visible. In the TabPFN panel, Figure 8(b), a mask must reach recall above roughly 0.8 before it is predicted to beat the all-feature baseline. This is a hard training regime. Without an explicit penalty for false positives or mask size, a learner can collapse to selecting nearly all variables. The shape of the region is precisely why exact F1 against B is not the right objective. F1 scores every error alike, whereas the reward map distinguishes errors by their predictive cost. It also shows that the downstream regressor decides whether a blanket helps. This is the bridge from diagnosis to the research directions of Section 7.

6.3 Beyond minimality

Layered blankets and the prediction gain map converge on the same revision of the target. Theorem 2.2 shows that $B(Y)$ is the minimal graphical sufficient set: no proper subset of $B(Y)$ is Bayes sufficient. But the theorem does not rule out Bayes-sufficient feature sets that lie outside $B(Y)$. Proxy or substitute variables that are not in the boundary can still carry equivalent predictive information, and Theorem 5.2 showed that any superset of $B(Y)$ preserves the population conditional. For prediction, minimality is a convenience rather than a requirement. A controlled superset of the boundary keeps the population conditional intact, and Section 6.2 shows that a wide band of such supersets still beats the full feature set. The prediction-aligned object is therefore not the singleton $B(Y)$ but a neighborhood around it.

Figure 9 sketches that neighborhood. The exact boundary is the innermost set. The second layer, mixed-layer masks, and an outer shell of proxy variables all sit close by, and each trades a little finite-sample efficiency for robustness to recall errors. The shell is not noise. In causal inference, proxy variables outside the minimal boundary carry information about latent or unmeasured causes, and are valuable precisely when boundary variables are missing or noisy [20, 39]. The operative question is no longer “did we recover $B(Y)$?” but “which set in this neighborhood does a given regressor want?” Section 7 turns this question into concrete research directions.

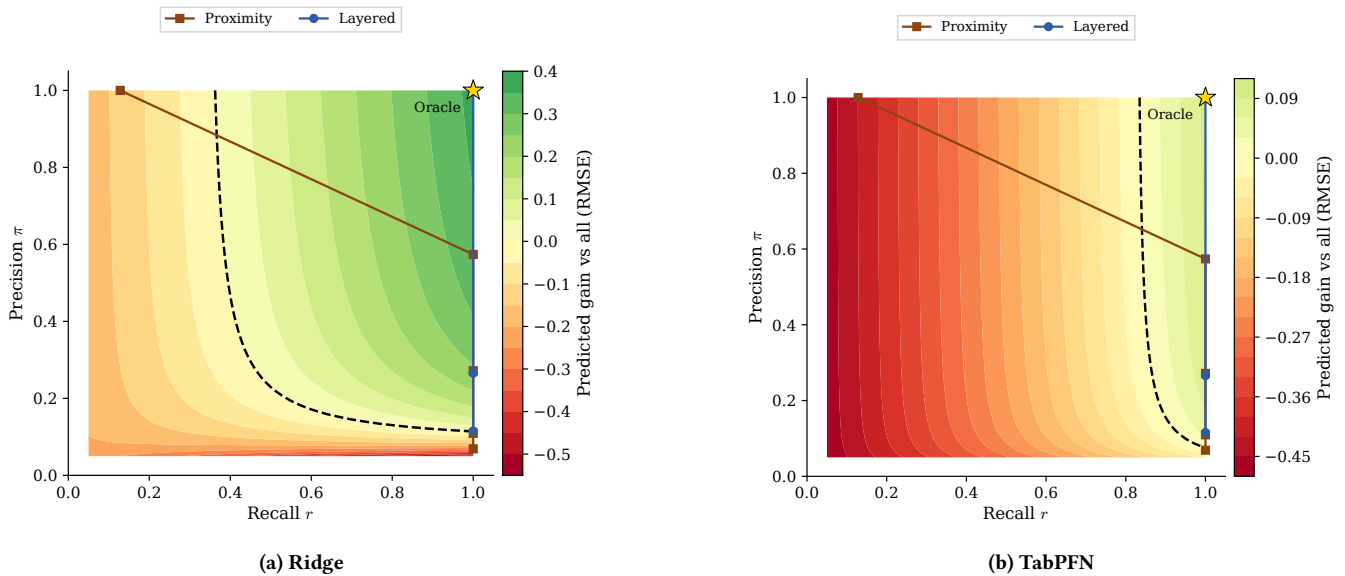


Figure 8: Prediction gain maps for Ridge and TabPFN. The axes are mask precision and recall against the oracle boundary; the color scale is predicted RMSE gain over the all-feature baseline. The zero contour separates masks that help from masks that hurt. Overlaid trajectories trace layered blankets (blue) and target-proximity masks (brown).

7 Implications

The three failure mechanisms of Section 5 are not dead ends. Each points to a way forward, and both directions below reuse a resource SCM3K made explicit. A synthetic SCM prior carries the ground-truth boundary $B(Y)$ alongside the data, a supervision signal that real observational tables never provide.

7.1 Scaling Markov-boundary estimation

The scalability failure of Section 5.1 is structural. A constraint-based estimator pays an $O(F^d)$ conditional-independence search for every new dataset. That cost is unavoidable only if the search is repeated per dataset, and it need not be. Tabular foundation models such as TabPFN and TabICL are already pre-trained on millions of synthetic tasks [11, 22, 27]. When those tasks are generated from SCMs, each one carries not just a table and a target but the target’s Markov boundary and the generating graph. The boundary is free supervision sitting unused in the prior.

This suggests pre-training a tabular model with a boundary-prediction head alongside the regression head, under a joint objective

$$\mathcal{L} = \mathcal{L}_{\text{pred}}(\hat{y}, y) + \lambda \mathcal{L}_{\text{mask}}(\hat{m}, B). \quad (16)$$

At inference the model returns a prediction together with an amortized boundary estimate, and the combinatorial search has been paid once, during pre-training, rather than once per dataset. Causal foundation models already make the analogous move for causal-effect estimation, training on SCM-generated tasks and reusing the learned prior at test time [3, 15, 30]. The architecture is the same, and only the supervision target changes. The asymmetry of Section 5.2 should be written directly into $\mathcal{L}_{\text{mask}}$ as a recall-weighted penalty, so the estimator is discouraged from dropping boundary features in the first place.

7.2 Synergizing blanket and prediction

Scaling the estimator does not by itself remove the objective mismatch of Section 5.2. Structural recovery and prediction remain different targets. The deeper fix is to stop treating boundary discovery as an unsupervised pre-processing step and let prediction loss inform it. Treating the mask m as a latent variable gives the factorization

$$P(y, m | D) = P(y | m, D) P(m | D), \quad (17)$$

in which the predictor and the mask are learned together rather than in sequence.

In that loop the two objectives reinforce each other. Prediction loss supervises $P(m | D)$ and supplies the signal that exact-recovery metrics miss. It identifies which mask errors actually cost accuracy. A structural prior on $P(m | D)$ keeps the mask anchored to the Markov boundary instead of collapsing onto whatever columns happen to help in-sample. The prediction gain map of Section 6.2 is a first sketch of the region such a loop should aim for. It is the band of precision and recall pairs whose masks are predicted to beat the full feature set. A co-trained mask need not recover $B(Y)$ exactly. It needs to land inside that band, and Section 6 shows the band is wide enough to make that a realistic target.

8 Related Work

Markov blanket discovery. Markov blanket discovery can be viewed as the local version of causal discovery. Full-graph methods recover a DAG, CPDAG, or equivalence class and then derive the target blanket from parents, children, and spouses. This connects blanket recovery to score-based search, such as GES

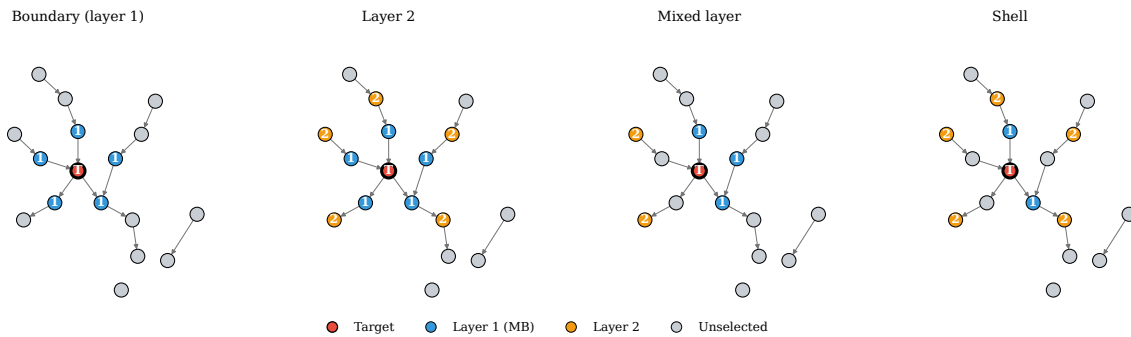


Figure 9: Why the exact boundary can be too exclusive. The exact boundary is the minimal sufficient set, but layer-2, mixed-layer, and shell masks can retain useful redundant or proxy variables. This distinction matters when prediction rewards recall more than exact minimality.

[6], and to constraint-based causal discovery, where conditional-independence tests determine the graph up to Markov equivalence [19, 32, 37]. These methods are designed primarily for structure. Their natural outputs are edges, equivalence classes, separating sets, or local neighborhoods.

Local blanket algorithms avoid full DAG recovery by searching directly around the target. Grow-Shrink expands and prunes a candidate blanket through conditional-independence tests [18]. HITON-MB and later local methods use related tests to identify parents, children, and spouses [1, 2, 34, 35]. Our study uses this literature as the natural baseline for the “estimate blanket, then predict” pipeline. The difference is the evaluation target. We ask whether the estimated blanket improves downstream regression, not whether it maximizes exact structural recovery.

Feature selection. The Markov blanket is also a classical target for feature selection. Under the usual graphical assumptions, it is the minimal feature set that preserves the target conditional, so it removes both irrelevant variables and variables made redundant by the boundary. Causality-based feature-selection work uses this idea to connect predictive parsimony, robustness, and interpretability [26, 41]. Recent work [40] extends Markov blankets to representation learning for domain generalization. In this view, causal structure is useful not only because it explains the data-generating process, but because it provides a principled feature mask for a supervised learner.

Our results refine that feature-selection story. The oracle boundary does improve prediction in wide, redundant regimes, but the advantage is finite-sample and regressor-dependent. Moreover, exact boundary identification is not the only goal relevant for prediction. False negatives and false positives have different costs, and many over-inclusive masks can preserve most of the oracle gain. This places our work between causal feature selection and empirical model selection. We keep the Markov boundary as the reference object, but we evaluate masks by prediction loss.

Tabular foundation models. Tabular foundation models use synthetic task priors to train predictors that can be reused across tabular datasets. TabPFN demonstrates this idea for small tabular tasks [11, 22], while TabICL extends the in-context-learning framing to larger tabular settings [27, 28]. In this paper, these models

are downstream regressors. They are not the main method or the main narrative device. Their role is useful precisely because they test whether the MB gap persists for modern tabular predictors that already encode strong prior information.

Causal foundation models make a parallel move for causal inference. They train on SCM-generated tasks and use the learned prior at test time for causal queries [3, 15, 30]. This line of work is relevant because SCM priors contain ground-truth blankets in addition to samples and graph structure. We do not propose a causal or tabular foundation model here. Instead, our results suggest a future training paradigm. Use the blanket information available in SCM priors to learn prediction-aligned feature masks jointly with prediction.

9 Conclusion

Our main evidence is simulated. SCM3K is broad across feature counts, graph densities, and six SCM families, but real-world validation remains necessary [4]. Good candidates include ARTH150, a 107-node Gaussian linear network [23, 31], and causalAssembly, a 98-node industrial assembly-line process [8]. DREAM4 size-100 and DREAM5 in-silico Net 1 provide continuous gene-regulatory networks [16, 17]. SynTREN provides configurable continuous sub-networks from real transcriptional networks [36]. A second limitation is that regressors are evaluated under a fixed protocol rather than fully fine-tuned per dataset or cohort. A third limitation is scope. We study regression with RMSE/MSE losses, not classification. Classification may interact with boundary size, redundancy, and mask errors differently.

Markov boundaries are useful for understanding when feature parsimony improves tabular prediction. The exact boundary is the minimal population-sufficient feature set, and the oracle gap is real in the high-dimensional redundant regime. But exact unsupervised boundary recovery is too narrow as a prediction objective. Prediction needs masks that preserve boundary information, control redundant features according to the downstream regressor, and scale to the regime where the oracle gap is visible. The central lesson is therefore not that every predictor should recover the exact Markov boundary. It is that Markov boundaries expose the structure that future prediction-aligned feature selection should learn to use.

References

- [1] Constantin F Aliferis, Alexander Statnikov, Ioannis Tsamardinos, Subramani Mani, and Xenofon D Koutsoukos. 2010. Local causal and Markov blanket induction for causal discovery and feature selection for classification part I: Algorithms and empirical evaluation. *Journal of Machine Learning Research* 11 (2010), 171–234.
- [2] Constantin F Aliferis, Ioannis Tsamardinos, and Alexander Statnikov. 2003. H1-TON: a novel Markov Blanket algorithm for optimal variable selection. In *AMIA annual symposium proceedings*, Vol. 2003. 21.
- [3] Vahid Balazadeh, Hamidreza Kamkari, Valentin Thomas, Junwei Ma, Bingru Li, Jesse C. Cresswell, and Rahul Krishnan. 2026. CausalPFN: Amortized Causal Effect Estimation via In-Context Learning. In *The Thirty-ninth Annual Conference on Neural Information Processing Systems*. <https://openreview.net/forum?id=RblaNjGx8C>
- [4] Philippe Brouillard, Chandler Squires, Jonas Wahl, Konrad K'ording, Karen Sachs, Alexandre Drouin, and Dhanya Sridhar. 2025. The Landscape of Causal Discovery Data: Grounding Causal Discovery in Real-World Applications. In *Proceedings of the Fourth Conference on Causal Learning and Reasoning (Proceedings of Machine Learning Research, Vol. 275)*, Biwei Huang and Mathias Drton (Eds.), PMLR, 834–873. <https://proceedings.mlr.press/v275/brouillard25a.html>
- [5] Tianqi Chen and Carlos Guestrin. 2016. XGBoost: A Scalable Tree Boosting System. In *Proceedings of the 22nd ACM SIGKDD International Conference on Knowledge Discovery and Data Mining (San Francisco, California, USA) (KDD '16)*. Association for Computing Machinery, New York, NY, USA, 785–794. doi:10.1145/2939672.2939785
- [6] David Maxwell Chickering. 2003. Optimal structure identification with greedy search. *J. Mach. Learn. Res.* 3, null (March 2003), 507–554. doi:10.1162/153244303321897717
- [7] Paul Erdős and Alfréd Rényi. 1960. On the evolution of random graphs. *Publications of the Mathematical Institute of the Hungarian Academy of Sciences* 5 (1960), 17–61.
- [8] Konstantin Göbler, Tobias Windisch, Mathias Drton, Tim Pchynski, Martin Roth, and Steffen Sonntag. 2024. causalAssembly: Generating Realistic Production Data for Benchmarking Causal Discovery. In *Proceedings of the Third Conference on Causal Learning and Reasoning (Proceedings of Machine Learning Research, Vol. 236)*, Francesco Locatello and Vanessa Didelez (Eds.), PMLR, 609–642. <https://proceedings.mlr.press/v236/gobler24a.html>
- [9] Trevor Hastie, Robert Tibshirani, and Jerome Friedman. 2009. *The Elements of Statistical Learning: Data Mining, Inference, and Prediction* (2 ed.). Springer, New York, NY. doi:10.1007/978-0-387-84858-7
- [10] Arthur E. Hoerl and Robert W. Kennard. 1970. Ridge Regression: Biased Estimation for Nonorthogonal Problems. *Technometrics* 12, 1 (1970), 55–67. arXiv:<https://doi.org/10.1080/00401706.1970.10488634> doi:10.1080/00401706.1970.10488634
- [11] Noah Hollmann, Samuel Müller, Katharina Eggensperger, and Frank Hutter. 2023. TabPFN: A Transformer That Solves Small Tabular Classification Problems in a Second. In *The Eleventh International Conference on Learning Representations*. https://openreview.net/forum?id=cp5PvcI6w8_
- [12] Kurt Hornik, Maxwell Stinchcombe, and Halbert White. 1989. Multilayer feed-forward networks are universal approximators. *Neural Networks* 2, 5 (1989), 359–366. doi:10.1016/0893-6080(89)90020-8
- [13] Daphne Koller and Nir Friedman. 2009. *Probabilistic Graphical Models: Principles and Techniques - Adaptive Computation and Machine Learning*. The MIT Press.
- [14] Nan M. Laird and James H. Ware. 1982. Random-Effects Models for Longitudinal Data. *Biometrics* 38, 4 (1982), 963–974. <http://www.jstor.org/stable/2529876>
- [15] Yuchen Ma, Dennis Frauen, Emil Javurek, and Stefan Feuerriegel. 2026. Foundation Models for Causal Inference via Prior-Data Fitted Networks. In *The Fourteenth International Conference on Learning Representations*. <https://openreview.net/forum?id=d2L1ndOKjq>
- [16] Daniel Marbach, James C Costello, Robert Küffner, Nicole M Vega, Robert J Prill, Diogo M Camacho, Kyle R Allison, Manolis Kellis, James J Collins, et al. 2012. Wisdom of crowds for robust gene network inference. *Nature methods* 9, 8 (2012), 796–804.
- [17] Daniel Marbach, Robert J. Prill, Thomas Schaffter, Claudio Mattiussi, Dario Floreano, and Gustavo Stolovitzky. 2010. Revealing strengths and weaknesses of methods for gene network inference. *Proceedings of the National Academy of Sciences* 107, 14 (2010), 6286–6291. arXiv:<https://www.pnas.org/doi/pdf/10.1073/pnas.0913357107> doi:10.1073/pnas.0913357107
- [18] Dimitris Margaritis and Sebastian Thrun. 1999. Bayesian Network Induction via Local Neighborhoods. In *Advances in Neural Information Processing Systems*, S.olla, T. Leen, and K. Müller (Eds.), Vol. 12. MIT Press. https://proceedings.neurips.cc/paper_files/paper/1999/file/5d79099cdf499f12b79770834c0164a-Paper.pdf
- [19] Christopher Meek. 1995. Causal inference and causal explanation with background knowledge. *Proceedings of the Eleventh Conference on Uncertainty in Artificial Intelligence* (1995), 403–410.
- [20] Wang Miao, Zhi Geng, and Eric J Tchetgen Tchetgen. 2018. Identifying causal effects with proxy variables of an unmeasured confounder. *Biometrika* 105, 4 (12 2018), 987–993. arXiv:<https://academic.oup.com/biomet/article-pdf/105/4/987/27121264/asy038.pdf> doi:10.1093/biomet/asy038
- [21] Samuel Müller, Noah Hollmann, Sebastian Pineda Arango, Josif Grabocka, and Frank Hutter. 2022. Transformers Can Do Bayesian Inference. In *International Conference on Learning Representations*. <https://openreview.net/forum?id=KSugKcbNf9>
- [22] Samuel Müller, Arik Reuter, Noah Hollmann, David Rügamer, and Frank Hutter. 2025. Position: The Future of Bayesian Prediction Is Prior-Fitted. In *Proceedings of the 42nd International Conference on Machine Learning (Proceedings of Machine Learning Research, Vol. 267)*. PMLR, Vancouver, Canada. <https://proceedings.mlr.press/v267/muller25d.html>
- [23] Rainer Opgen-Rhein and Korbinian Strimmer. 2007. From correlation to causation networks: a simple approximate learning algorithm and its application to high-dimensional plant gene expression data. *BMC systems biology* 1, 1 (2007), 37.
- [24] Judea Pearl. 1988. *Probabilistic Reasoning in Intelligent Systems: Networks of Plausible Inference*. Morgan Kaufmann Publishers Inc., San Francisco, CA, USA.
- [25] Judea Pearl. 2009. *Causality: Models, Reasoning and Inference* (2nd ed.). Cambridge University Press, USA.
- [26] Jonas Peters, Dominik Janzing, and Bernhard Schölkopf. 2017. *Elements of Causal Inference: Foundations and Learning Algorithms*. MIT Press, Cambridge, MA.
- [27] Jingang Qu, David Holzmüller, Gaël Varoquaux, and Marine Le Morvan. 2025. TabICL: A Tabular Foundation Model for In-Context Learning on Large Data. In *Proceedings of the 42nd International Conference on Machine Learning (Proceedings of Machine Learning Research, Vol. 267)*. PMLR, Vancouver, Canada, 50817–50847. <https://proceedings.mlr.press/v267/qu25d.html>
- [28] Jingang Qu, David Holzmüller, Gaël Varoquaux, and Marine Le Morvan. 2026. TabICLv2: A better, faster, scalable, and open tabular foundation model. arXiv:2602.11139 [cs.LG] <https://arxiv.org/abs/2602.11139>
- [29] Alexander Reisach, Christof Seiler, and Sebastian Weichwald. 2021. Beware of the simulated dag! causal discovery benchmarks may be easy to game. *Advances in Neural Information Processing Systems* 34 (2021), 27772–27784.
- [30] Jake Robertson, Arik Reuter, Siyuan Guo, Noah Hollmann, Frank Hutter, and Bernhard Schölkopf. 2025. Do-PFN: In-Context Learning for Causal Effect Estimation. arXiv:2506.06039 [cs.LG] <https://arxiv.org/abs/2506.06039>
- [31] Marco Scutari. 2010. Learning Bayesian networks with the bnlearn R package. *Journal of statistical software* 35 (2010), 1–22.
- [32] Peter Spirtes, Clark Glymour, and Richard Scheines. 2000. *Causation, Prediction, and Search* (2 ed.). MIT Press, Cambridge, MA.
- [33] Robert Tibshirani. 1996. Regression Shrinkage and Selection Via the Lasso. *Journal of the Royal Statistical Society: Series B (Methodological)* 58, 1 (01 1996), 267–288. doi:10.1111/j.2517-6161.1996.tb02080.x
- [34] Ioannis Tsamardinos, Constantin F. Aliferis, and Alexander Statnikov. 2003. Algorithms for Large Scale Markov Blanket Discovery. In *Proceedings of the Sixteenth International Florida Artificial Intelligence Research Society Conference (FLAIRS 2003)*. AAAI Press, Menlo Park, CA, 376–381. <https://aaai.org/papers/flairs-2003-073/>
- [35] Ioannis Tsamardinos, Laura E Brown, and Constantin F Aliferis. 2006. The max-min hill-climbing Bayesian network structure learning algorithm. *Machine Learning* 65, 1 (2006), 31–78.
- [36] Tim Van den Bulcke, Koenraad Van Leemput, Bart Naudts, Piet van Remortel, Hongwu Ma, Alain Verschoren, Bart De Moor, and Kathleen Marchal. 2006. SYNTRen: a generator of synthetic gene expression data for design and analysis of structure learning algorithms. *BMC bioinformatics* 7, 1 (2006), 43.
- [37] Thomas Verma and Judea Pearl. 1990. Equivalence and synthesis of causal models. *Proceedings of the Sixth Conference on Uncertainty in Artificial Intelligence* (1990), 220–227.
- [38] Jeffrey M. Wooldridge. 2010. *Econometric Analysis of Cross Section and Panel Data*. The MIT Press. <http://www.jstor.org/stable/j.ctt5hchfr>
- [39] Liyuan Xu, Heishiro Kanagawa, and Arthur Gretton. 2021. Deep Proxy Causal Learning and its Application to Confounded Bandit Policy Evaluation. In *Advances in Neural Information Processing Systems*, M. Ranzato, A. Beygelzimer, Y. Dauphin, P.S. Liang, and J. Wortman Vaughan (Eds.), Vol. 34. Curran Associates, Inc., 26264–26275. https://proceedings.neurips.cc/paper_files/paper/2021/file/dcf3219715a7c9cd9286f19db46f2384-Paper.pdf
- [40] Naiyu Yin, Hanjing Wang, Yue Yu, Tian Gao, Amit Dhurandhar, and Qiang Ji. 2024. Integrating Markov blanket discovery into causal representation learning for domain generalization. In *European Conference on Computer Vision*. Springer, 271–288.
- [41] Kui Yu, Lin Liu, Jiuyong Li, Weiping Ding, and Thuc Duy Le. 2020. Causality-based feature selection: Methods and evaluations. *Comput. Surveys* 53, 5 (2020), 1–36.